

## Supporting Information

### High-Sensitivity Rheo-NMR Spectroscopy for Protein Studies

Daichi Morimoto<sup>†</sup>, Erik Walinda<sup>‡</sup>, Naoto Iwakawa<sup>†</sup>, Mayu Nishizawa<sup>†</sup>, Yasushi Kawata<sup>#</sup>, Akihiko Yamamoto<sup>§</sup>, Masahiro Shirakawa<sup>†</sup>, Ulrich Scheler<sup>¶</sup>, and Kenji Sugase<sup>\*, †</sup>

<sup>†</sup>Department of Molecular Engineering, Graduate School of Engineering, Kyoto University, Kyoto-Daigaku Katsura, Nishikyo-ku, Kyoto 615-8510, Japan

<sup>‡</sup>Department of Molecular and Cellular Physiology, Graduate School of Medicine, Kyoto University, Yoshida Konoe-cho, Sakyo-ku, Kyoto 606-8501, Japan

<sup>#</sup>Department of Chemistry and Biotechnology, Graduate School of Engineering, Tottori University, 4-101 Koyama-cho Minami, Tottori 680-8552, Japan

<sup>§</sup>Bruker BioSpin K.K., 3-9 Moriya-cho, Kanagawa-ku, Yokohama, Kanagawa 221-0022, Japan

<sup>¶</sup>Leibniz-Institut für Polymerforschung Dresden e.V., Hohe Strasse 6, D-01069 Dresden, Germany

**Corresponding Author:** \* sugase@moleng.kyoto-u.ac.jp

### Table of Contents

#### Supplementary Methods

- Flow gradient in the Rheo-NMR experiment.
- NMR measurements.
- NMR relaxation analysis.
- Real-time Rheo-NMR measurements.
- Comparison of sensitivity between standard and Rheo-NMR setting conditions.
- Calculation of the order parameter and the rotational diffusion tensor.

#### Supplementary Figures

- Figure S1. Construction of the Rheo-NMR instrument in this study.
- Figure S2. Chemical shift differences between static and sheared ubiquitin.
- Figure S3. Shear-dependent peak volume decrease in the real-time NMR experiments.
- Figure S4. Chemical shift differences between static and sheared M1-linked hexa-ubiquitin.
- Figure S5. Mapping of differences in the chemical shift of ubiquitin residues between static and sheared conditions.

#### Supplementary Table

- Table S1. Rotational diffusion tensor parameters for static and sheared ubiquitin.

#### References

## Supplementary Methods

**Flow gradient in the Rheo-NMR experiment.** The flow gradient of the fluid was obtained, and the flow velocity  $v_r$  at the radius  $r$  from the center was calculated by the following equation<sup>1</sup>:

$$v_r = r\Omega \frac{R_i^{-2} - r^{-2}}{R_i^{-2} - R_o^{-2}}, \quad (1)$$

where  $\Omega$  is the angular frequency of the spinner,  $R_i$  is the outer radius of the inner glass stick, and  $R_o$  is the inner radius of the outer NMR tube. The shear rate  $\dot{\gamma}_r$  at a distance  $r$  from the center was estimated by the following equation<sup>1</sup>:

$$\dot{\gamma}_r = \frac{2\Omega r^{-2}}{R_i^{-2} - R_o^{-2}}. \quad (2)$$

The average shear rate  $\langle \dot{\gamma} \rangle$  was estimated by the following equation<sup>2</sup>:

$$\langle \dot{\gamma} \rangle = \frac{\int_{R_i}^{R_o} r \dot{\gamma} dr}{\int_{R_i}^{R_o} r dr} = \frac{4\Omega \ln(R_i^{-1} R_o)}{R_i^2 R_o^2 (R_i^{-2} - R_o^{-2})^2}. \quad (3)$$

In the case of a spinning frequency of 35 Hz, the flow velocity  $v_r$  and the shear rate  $\dot{\gamma}_r$  were calculated as the respective range of 0–0.45 m s<sup>-1</sup> and 950–510 s<sup>-1</sup>, corresponding to  $R_i \leq r \leq R_o$ , and the average shear rate  $\langle \dot{\gamma} \rangle$  was 680 s<sup>-1</sup>.

**NMR measurements.** The proteins were dissolved in buffer containing 20 mM potassium phosphate, 5 mM KCl, 1 mM EDTA, 150 mM NaCl, and 10% D<sub>2</sub>O at pH 6.8. The protein concentration of ubiquitin and that of ubiquitin subunits of M1-linked hexa-ubiquitin were 0.5 mM. For the <sup>15</sup>N longitudinal ( $R_1$ ) relaxation experiment, a series of spectra with relaxation delays of 10, 30, 170, 290, 490, 690, and 990 milliseconds were measured. For the <sup>15</sup>N transverse

( $R_2$ ) relaxation experiment, a series of spectra with relaxation delays of 15.68, 31.36, 47.04, 62.72, 78.40, 94.08, 109.76, and 141.12 milliseconds were acquired. All relaxation data were acquired in an interleaved manner. To ensure adequate longitudinal relaxation between acquisitions, the recycle delay was set to 5 seconds for the  $^1\text{H}$ - $^{15}\text{N}$  NOE measurements and 3 seconds for the  $R_1$ , and  $R_2$  relaxation measurements. Data processing was performed in NMRPipe<sup>3</sup> or TopSpin (Bruker BioSpin) and the data were analyzed by CcpNmr Analysis<sup>4</sup> or TopSpin.  $^1\text{H}$ - $^{15}\text{N}$  resonance assignments and  $^1\text{H}$ - $^{13}\text{C}$  resonance assignments for human ubiquitin were derived from entry 17769 in the Biological Magnetic Resonance Bank. Because the spectrum of hexa-ubiquitin showed a peak pattern similar to that of monomeric ubiquitin, the chemical shift of each cross-peak in the spectrum of hexa-ubiquitin was estimated as the average chemical shift of six ubiquitin subunits.

**NMR relaxation analysis.** In the  $^{15}\text{N}$  longitudinal ( $R_1$ ) and transverse ( $R_2$ ) relaxation experiments, the signal intensities  $I(t)$  of each peak with different relaxation delays  $t$  were fitted to the equation  $I(t) = I(0)\exp(-R_\alpha t)$ , yielding the relaxation rate  $R_\alpha$ , where  $\alpha = 1$  or 2. Fitting was performed by using the program GLOVE.<sup>5</sup>  $^1\text{H}$ - $^{15}\text{N}$  heteronuclear NOE (hnNOE) values were calculated by the equation: (hnNOE value) =  $I_{\text{sat}} / I_{\text{eq}}$ , where  $I_{\text{sat}}$  and  $I_{\text{eq}}$  are the peak intensities with and without proton saturation, respectively. The values represent the average of two independent experiments. Errors in the  $R_1$  and  $R_2$  relaxation rates were calculated by the Monte Carlo method,<sup>5</sup> and errors in the hnNOE values were estimated by the standard deviation of two experiments.

**Real-time Rheo-NMR measurements.**  $^1\text{H}$ - $^{15}\text{N}$  and  $^1\text{H}$ - $^{13}\text{C}$  HSQC spectra were alternately measured in the real-time experiment. As a control static condition, HSQC spectra were acquired in the Rheo-NMR instrument without spinning. The real-time NMR measurements under the sheared condition were started immediately after the spinning began. The time point of each spectrum was estimated to be the middle point between the start and end time points.

**Comparison of sensitivity between standard and Rheo-NMR setting conditions.**  $^1\text{H}$ - $^{15}\text{N}$  HSQC spectra ( $^1\text{H}$ : from 9.60 to 6.00 ppm;  $^{15}\text{N}$ : from 134 to 102 ppm) of 0.1 mM ubiquitin in the standard and Rheo-NMR setting conditions were acquired. The sample volume was 0.3 ml. The protein was dissolved in buffer containing 20 mM potassium phosphate, 5 mM KCl, 1 mM EDTA, 50 mM NaCl, and 10%  $\text{D}_2\text{O}$  at pH 6.8. The number of scans and receiver gain of HSQC measurements were identical in the two experimental conditions. The obtained average signal-to-noise of peaks in the standard and Rheo-NMR setting conditions was 128.9 and 77.8, respectively.

**Calculation of the order parameter and the rotational diffusion tensor.** The order parameters and rotational diffusion tensor of static and sheared ubiquitin were calculated from respective  $^{15}\text{N}$   $R_1$ ,  $R_2$  relaxation rates and  $\text{hnNOE}$  values by using the program ROTDIF.<sup>6</sup> The NMR structure of ubiquitin (PDB database number 1D3Z) was used for calculation. The data for static and sheared ubiquitin were fitted to the axially-symmetric model. The tensor parameters are listed in Table 1.

## Supplementary Figures

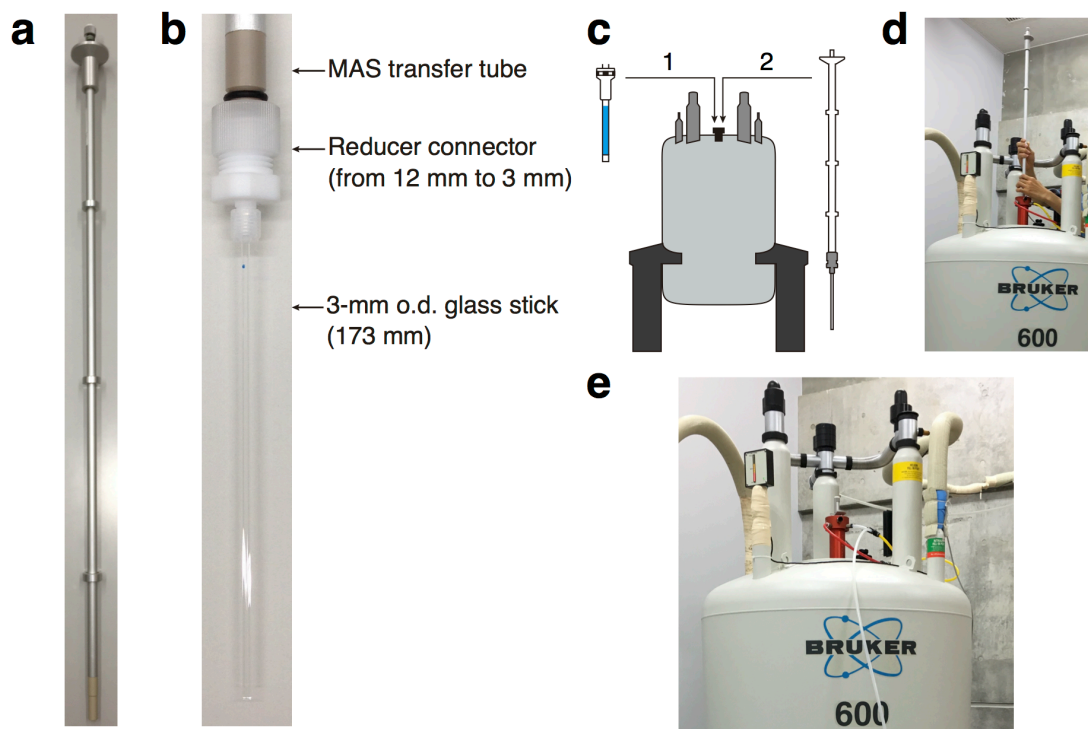


**Figure S1. Construction of the Rheo-NMR instrument in this study.** **a**, A magic-angle-spinning (MAS) transfer tube that fits to an upper shim stack of our NMR instrument. **b**, A 3-mm outer diameter glass stick was connected to the bottom of the MAS transfer tube via a 12-mm-to-3-mm reducer connector. **c**, A sample of 0.3 ml was prepared in a 5-mm outer diameter NMR tube with a ceramic spinner. The NMR tube was then inserted into an NMR instrument using air flowing for inserting/ejecting and subsequently the MAS transfer tube was slowly inserted (**d**). **e**, An NMR instrument equipped with the Rheo-NMR accessory.

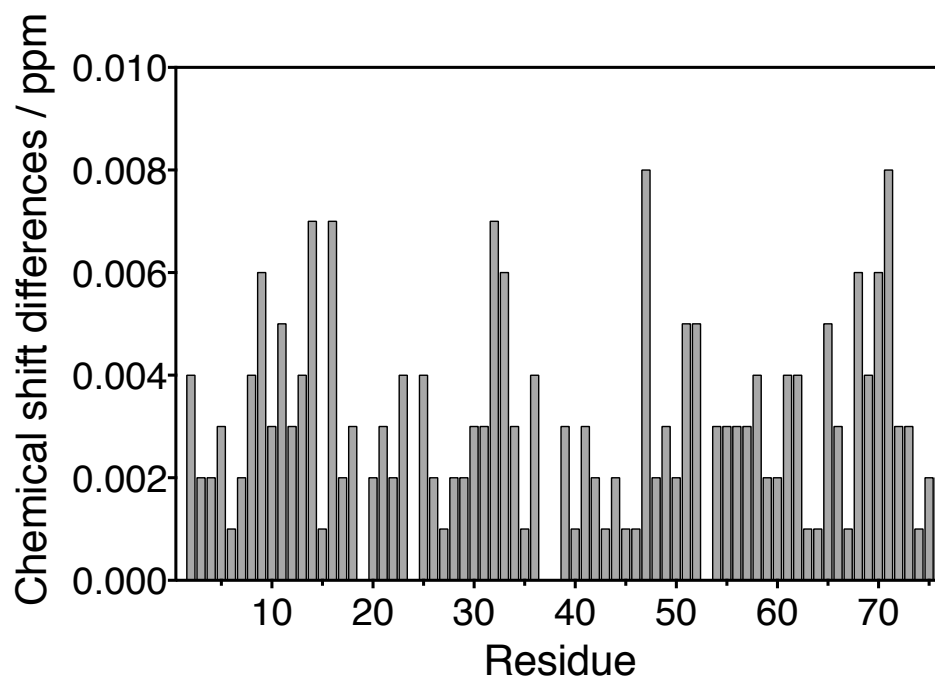


**Figure S2. Chemical shift differences between static and sheared ubiquitin.** Chemical shift differences were obtained from the equation  $\Delta\delta_{wt} = [\Delta\delta_{HN}^2 + (\Delta\delta_N / 5)^2]^{0.5}$ , where  $\Delta\delta_{HN}$  and  $\Delta\delta_N$  are the  $^1\text{H}$  and  $^{15}\text{N}$  chemical shift changes between static and sheared ubiquitin at a spinning frequency of 35 Hz.

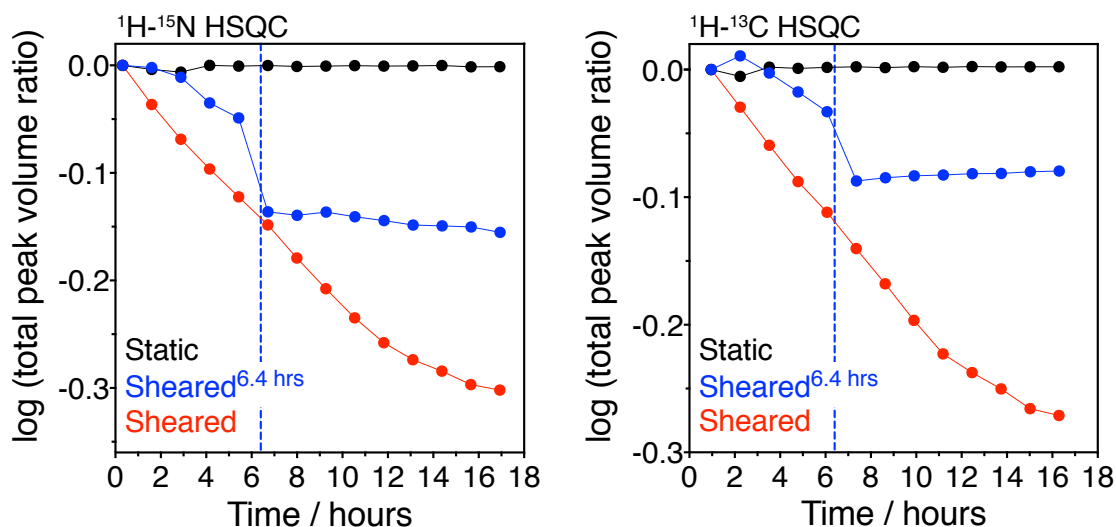


**Figure S3. Shear-dependent peak volume decrease in the real-time NMR experiments.**

Real-time NMR profiles under static (black) and sheared conditions for 17 hours (red) were obtained from the total peak volume of peaks in the respective spectra. The real-time NMR profiles were also obtained while shear flow was applied to hexa-ubiquitin for 6.4 hours and was then stopped (blue). The vertical dashed blue line shows the time when the spinning was stopped ( $t = 6.4$  hours). The total peak volume of peaks in the  $^1\text{H}$ - $^{15}\text{N}$  HSQC spectra (Left,  $^1\text{H}$ : from 9.60 to 6.00 ppm;  $^{15}\text{N}$ : from 134 to 102 ppm) and  $^1\text{H}$ - $^{13}\text{C}$  HSQC spectra (Right,  $^1\text{H}$ : from 3.28 to -0.35 ppm;  $^{13}\text{C}$ : from 42.20 to 5.50 ppm) of hexa-ubiquitin was calculated. The ratio of peak volume at each time point to that at the first point ( $t = 0.32$  and  $0.96$  hours in  $^1\text{H}$ - $^{15}\text{N}$  and  $^1\text{H}$ - $^{13}\text{C}$  HSQC data, respectively) is shown. Due to the difference in magnetic field homogeneity between the static and sheared conditions, the peak volume after the stop of the spinning ( $t > 6.4$  hours) was normalized by the peak volume obtained before the spinning ( $t = 0$ ).

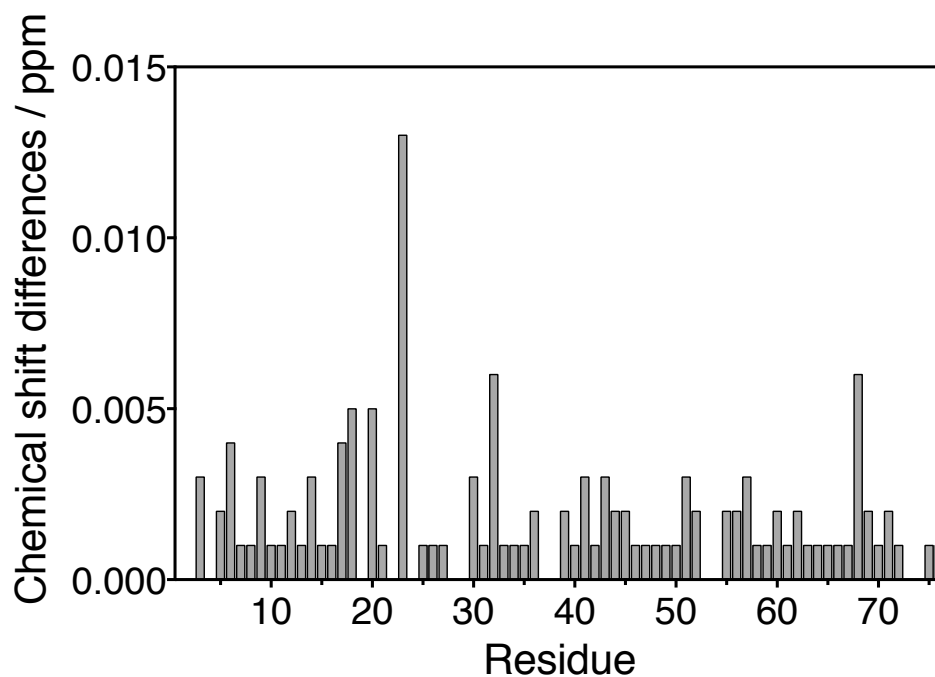


**Figure S4. Chemical shift differences between static and sheared M1-linked hexa-ubiquitin.**

Chemical shift differences were obtained from the equation  $\Delta\delta_{\text{wt}} = [\Delta\delta_{\text{HN}}^2 + (\Delta\delta_{\text{N}} / 5)^2]^{0.5}$ , where  $\Delta\delta_{\text{HN}}$  and  $\Delta\delta_{\text{N}}$  are the  $^1\text{H}$  and  $^{15}\text{N}$  chemical shift changes between static and sheared hexa-ubiquitin at a spinning frequency of 35 Hz for 17 hours.



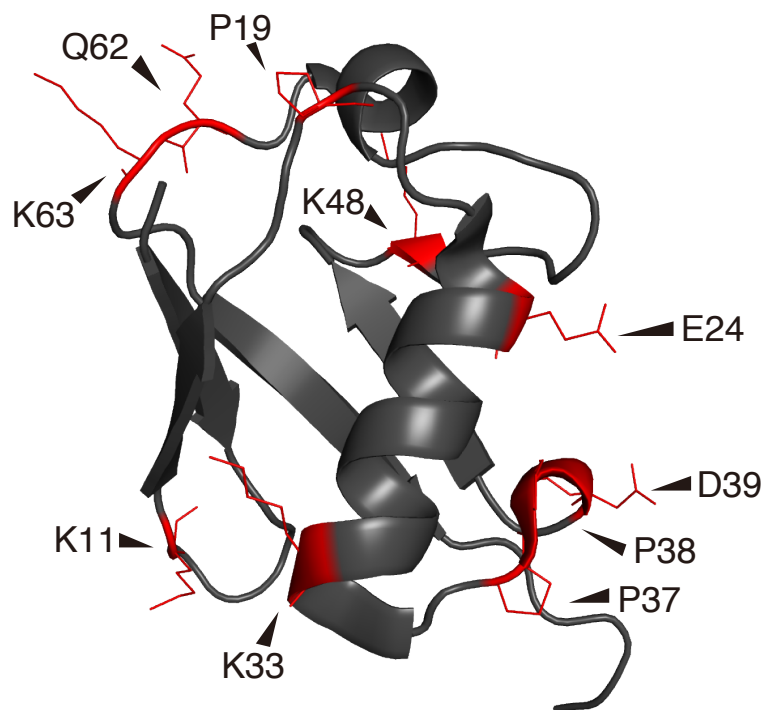


**Figure S5. Mapping of differences in the chemical shift of ubiquitin residues between static and sheared conditions.** During the fibril formation of hexa-ubiquitin, differences in chemical shift were observed for all indicated residues. The structure was drawn from PDB database entry 1D3Z.

**Table S1. Rotational diffusion tensor parameters for static and sheared ubiquitin.**

	$D_{\perp} / 10^7 \text{ s}^{-1}$	$D_{\parallel} / 10^7 \text{ s}^{-1}$	$\alpha / ^{\circ}$	$\beta / ^{\circ}$	$\tau_c / \text{ns}$	$\zeta$
Static	$3.52 \pm 0.04$	$4.43 \pm 0.05$	$108 \pm 11$	$157 \pm 3$	$4.36 \pm 0.02$	$1.26 \pm 0.03$
Sheared	$3.52 \pm 0.03$	$4.56 \pm 0.08$	$128 \pm 15$	$157 \pm 2$	$4.31 \pm 0.02$	$1.30 \pm 0.05$

$D_{\perp}$  and  $D_{\parallel}$  are the respective perpendicular and parallel components of the rotational diffusion tensor;  $\alpha$ ,  $\beta$  are Euler angles;  $\tau_c$  is the overall correlation time; and  $\zeta$  is the anisotropy of the rotational diffusion tensor. Errors were estimated by the Monte Carlo method.

## References

1. McKelvey, J. M., *Polymer processing*. Wiley: New York, **1962**.
2. Maa, Y. F.; Hsu, C. C., *Biotechnol. Bioeng.* **1996**, *51* (4), 458-465.
3. Delaglio, F.; Grzesiek, S.; Vuister, G. W.; Zhu, G.; Pfeifer, J.; Bax, A., *J. Biomol. NMR* **1995**, *6* (3), 277-293.
4. Vranken, W. F.; Boucher, W.; Stevens, T. J.; Fogh, R. H.; Pajon, A.; Llinas, M.; Ulrich, E. L.; Markley, J. L.; Ionides, J.; Laue, E. D., *Proteins* **2005**, *59* (4), 687-696.
5. Sugase, K.; Konuma, T.; Lansing, J. C.; Wright, P. E., *J. Biomol. NMR* **2013**, *56* (3), 275-283.
6. Berlin, K.; Longhini, A.; Dayie, T. K.; Fushman, D., *J. Biomol. NMR* **2013**, *57* (4), 333-352.